Inorg. Chem. **2002**, *41*, 869–873

Structure-Directing Coordination Template Effect of Ethylenediamine in Formations of ZnS and ZnSe Nanocrystallites via Solvothermal Route

Zhao-Xiang Deng, Cheng Wang, Xiao-Ming Sun, and Ya-Dong Li*

Department of Chemistry and the Key Laboratory of Atomic & Molecular Nanosciences (Ministry of Education, China), Tsinghua University, Beijing, 100084, People's Republic of China

Received March 29, 2001

ZnS and ZnSe precursors (ZnS·0.5en and ZnSe·0.5en, en = ethylenediamine) were prepared via a solvothermal process using ethylenediamine as solvent. Phase-pure hexagonal wurtzite ZnS and ZnSe products were obtained by annealing the precursors in argon stream at temperatures above 350 °C. The role of ethylenediamine as a structure-directing coordination molecular template responsible for the morphologies of the annealed products was discussed. This work provided further insights into the solvent coordination molecular template (SCMT) mechanism previously proposed to explain the growth mechanism of CdE (E = S, Se, Te) nanorods in ethylenediamine (*Inorg. Chem.* **1999**, *38*, 1382). The as-prepared precursors as well as the annealed products were characterized by powder X-ray diffraction (XRD), transmission electron microscopy (TEM), infrared absorbance spectroscopy (IR), thermogravimetric analysis (TGA), X-ray fluorescence (XRF) analysis, and combustion analysis for C, N, H contents.

Introduction

The preparation of nanosized crystallites with different morphologies provides an opportunity to explore the evolutions of material properties with crystal structure, size, and shape. The fabrication of nanocrystals with controlled morphologies is always potentially important in the preparations of materials suitable for optoelectronic and luminescent applications.

A controlled synthetic method for one-dimensionally (1D) nanostructured materials is particularly interesting as 1D nanostuctures may serve as building blocks for many novel functional materials, which are currently the focus of considerable research interest.[1−17] The vapor−liquid−solid (VLS)[9−14] and the vapor−solid (VS) mechanism[18−21] for the growth of crystalline whisker or fiber at high temperature are widely known. A hydrothermal liquid−solid (LS) growth mechanism was proposed by Shi Erwei[22] and Masahiro.[23] Recently, Buhro proposed a solution−liquid−solid (SLS) mechanism[17] for the growth of III−V semiconductor fibers from organic solutions.

In our previous work for the synthesis of II−VI semiconductor nanorods by solvothermal route using enthylenediamine as liquid media, a solvent coordination molecular template (SCMT) mechanism was proposed.[24,25] However, attempts to prepare ZnE (E = S, Se) nanorods, which may

* To whom correspondence should be addressed. Telephone: 86-10-62772350. Fax: 86-10-62788765. E-mail: ydli@tsinghua.edu.cn.

(1) Dai, H.; Wong, E. W.; Lu, Y. Z.; Fan, S.; Lieber, C. M. *Nature* **1995**, *375*, 769.
(2) Yang, P. D.; Lieber, C. M. *Science* **1996**, *273*, 1836.
(3) Morales, A. M.; Lieber, C. M. *Science* **1998**, *279*, 208.
(4) Yazawa, M.; Koguchi, M.; Hiruma, K. *Appl. Phys. Lett.* **1991**, *58*, 1080.
(5) Yazawa, M.; Koguchi, M.; Hiruma, K. *Adv. Mater.* **1993**, *5*, 577.
(6) Han, W. Q.; Fan, S. S.; Li, Q. Q.; Hu, Y. D. *Science* **1997**, *277*, 1287.
(7) Huynh, W. U.; Peng, X. G.; Alivisato, A. P. *J. Am. Chem. Soc.* **1998**, *120*, 5343.
(8) Wang, W. Z.; Geng, Y.; Yan, P.; Liu, F. Y.; Xie, Y.; Qian, Y. T. *J. Am. Chem. Soc.* **1999**, *121*, 4062.
(9) Wagner, R. S.; Elhs, W. C. *Appl. Phys. Lett.* **1964**, *4*, 89.
(10) Glezie, P.; Schouler, M. C.; Gradelle, P.; Caillet, M. *J. Mater. Sci.* **1994**, *29* (6), 1576.
(11) Chang, W.; et al. *Nanostruct. Mater.* **1994**, *4* (5), 507.
(12) Koparanova, N.; Zlatev. Z.; Genchew, D.; et al. *J. Mater. Sci.* **1994**, *29*, 103.
(13) Givargizov, E. I.; Babasian, P. A. *J. Cryst. Growth* **1977**, *37*, 129.
(14) Toshitaka, O.; Masayuki, N. *J. Cryst. Growth* **1979**, *46*, 504.
(15) Braum, P. V.; Osenar, P.; Stupp, S. I. *Nature* **1996**, *380*, 325.
(16) Yang, J. P.; Meldrum, F. C.; Fendler, J. H. *J. Phys. Chem.* **1995**, *99*, 5500.
(17) Trentler, T. J.; Hichman, K. M.; Goel. S. C.; Viano, A. M.; Gibbons, P. C.; Buhro, W. E. *Science* **1995**, *270*, 1791.
(18) Frank, F. C. *Philos. Mag.* **1953**, *44*, 854.
(19) Iwao, Y.; Hajime, S. *J. Cryst. Growth* **1978**, *45*, 51.
(20) Inna, G.; Silver, S. M.; Deberah, A. H. U.S. Patent 4,948,766, Aug 14, 1990.
(21) Ishii, T.; Sekikawa Y.; et al. *J. Cryst. Growth* **1981**, *25*, 285.
(22) Erwei; et al. *Wuji Cailiao Xuebao (Chinese)* **1992**, *7* (3), 300.
(23) Masahiro, Y.; Hiroyuki, S.; Kengo, O.; et al. *J. Mater. Sci.* **1994**, *29*, 3399.

10.1021/ic0103502 CCC: $22.00
Published on Web 01/19/2002

have broad applications as direct band-gap semiconductors, luminescent and photocatalytic materials,[26−30] also employing ethylenediamine as the template agent failed.[31]

In a typical SCMT process, ethylenediamine acts as a template molecule which is incorporated into the inorganic framework first and then escapes from it to form nanocrystallites with desired morphologies. Although the SCMT mechanism was suggested and supported by successful preparations of rodlike CdE nonaphase, the role ethylenediamine plays in the structure-directing nucleation process is not very clear and thus needs further evidence.

In this work, we report an investigation on the role of ethylenediamine in the formations of the precursors to nanocrystalline ZnS and ZnSe. Powder X-ray diffraction (XRD), transmission electron microscopy (TEM), thermogravimetric analysis (TGA), IR absorbance spectroscopy, X-ray fluorescence spectroscopy (XRF), and combustion analysis were employed for structure and composition analysis.

Experimental Section

Synthesis. The synthesis of ZnS or ZnSe precursor was carried out by two different procedures: (1) appropriate amounts of zinc powder (99.99%) and sulfur powder (99.95%) or selenium powder (99.95%) were put into a Teflon-lined autoclave with a stainless steel shell and then the autoclave was filled with ethylenediamine to about 90% of its total capacity; (2) the same as 1 but using anhydrous $ZnCl_2$ (AR grade) as the zinc source instead of zinc powder. The autoclave was sealed and maintained at 180 °C for 18−24 h and then allowed to cool to room temperature naturally. Precipitates were collected and washed with deionized water and then alcohol repeatedly to remove inorganic and organic residues. The final products were dried in air at 50 °C for 3−4 h. To obtain phase-pure ZnS and ZnSe nanocrystallites, the as-prepared precursors were annealed separately under argon stream at 350, 600, and 800 °C for 2−3 h.

Characterization. Powder X-ray diffraction (XRD) patterns of all samples were measured on a Bruker D8-advance X-ray powder diffractometer with Cu Kα radiation ($\lambda = 1.5418$ Å). The operation voltage and current are 40 kV and 40 mA, respectively. XRD data were recorded with a resolution of 0.02° and a scan rate of 0.5 s/point. TEM images were taken with a Hitachi Model-800 transmission electron microscope using an accelerating voltage of 200 kV. TGA of the samples were conducted on a TGA-2050 (TA Corp.) thermogravimeter. Compositional analysis of the as-synthesized precursors and the annealed products were carried out on a Shimadzu XRF-1700 XRF spectrometer and a Carbo Erba 1106 elements analyzer. Infrared spectra of the samples were obtained on a Perkin-Elmer Spectrum GX FTIR spectrometer.

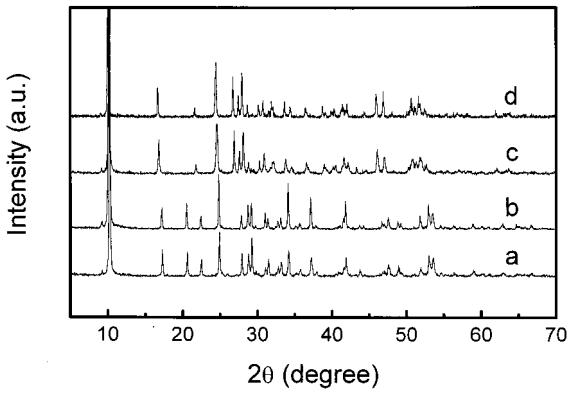

Figure 1. XRD patterns of the solvothermally synthesized ZnS and ZnSe precursors in ethylenediamine using different source agents for zinc: (a) Zn + S, (b) $ZnCl_2$ + S, (c) Zn + Se, and (d) $ZnCl_2$ + Se.

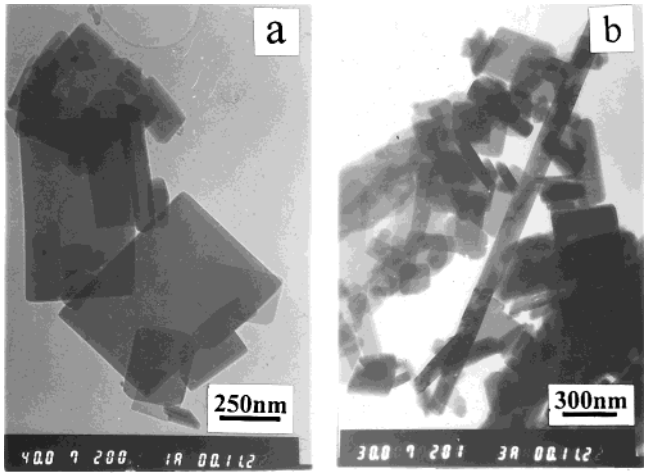

Figure 2. TEM images of the as-synthesized (a) ZnS and (b) ZnSe precursors.

Results and Discussion

Figure 1 shows the XRD results of the solvothermally prepared ZnS (Figure 1a,b) and ZnSe (Figure 1c,d) precursors. As one can seen from Figure 1, the precursors synthesized using different zinc agents have almost the same XRD patterns, indicating that the same products were obtained in synthetic procedures 1 and 2. The strong and sharp diffraction peaks appearing in the XRD diagrams have obvious relevance with the well-crystallized precursors. Unfortunately, these peaks cannot be indexed to any known phase of Zn, S, Se, ZnS, or ZnSe provided in the standard JCPDS cards. The likeness between the XRD patterns in Figure 1a,b and Figure 1c,d implies that these two precursors may have similar crystal structures. The shifts of the peak positions probably correspond to the different lattice constants of these two substances, due to the different atomic radii for S and Se.

TEM images of the two precursors are shown in Figure 2. As shown in the TEM pictures, both the ZnS and ZnSe precursors synthesized using different source materials for zinc have platelet morphologies. Selected area electron diffraction (SAED) of the platelike particles of ZnS precursor

(24) Li, Y. D.; Liao, H. W.; Ding, Y.; Qian, Y. T.; et al. *Chem. Mater*. **1998**, *10*, 2301.
(25) Li, Y. D.; Liao, H. W.; Ding, Y.; Fan, Y.; Zhang, Y.; Qian, Y. T. *Inorg. Chem*. **1999**, *38*, 1382.
(26) Xu, G. Q. *Langmuir* **1997**, *13*, 6427.
(27) Yin, H.; Wada, Y.; Kitamura, T.; Yanagida, S. *Environ. Sci. Technol*. **2001**, *35*, 227.
(28) Li, Y.; Ding, Y.; Zhang, Y.; Qian, Y. T. *J. Phys. Chem. Solids* **1999**, *60*, 13.
(29) Harris Liao, M. C.; Chang, Y. H.; Chen, Y. F.; Hsu, J. W.; Lin, J. M.; Chou, W. C. *Appl. Phys. Lett*. **1997**, *70*, 2256.
(30) Haase, M. A.; Baude, P. F.; Hafedorn, M. S.; Qiu, J.; DePuydt, J. M.; Cheng, H.; Guha, S.; Holfer, G. E.; Wu, B. J. *Appl. Phys. Lett*. **1993**, *63*, 2315.
(31) Li, Y. D.; Ding, Y.; Qian, Y. T.; et al. *Inorg. Chem*. **1998**, *37*, 2844.

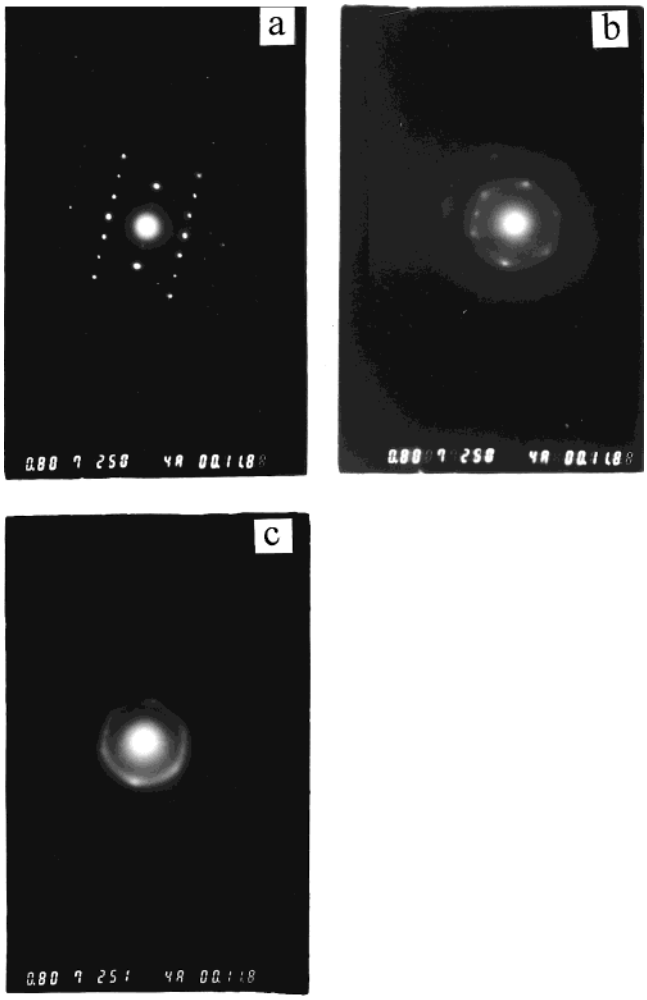

Figure 3. Evolution of the selected area electron diffraction (SAED) patterns (a → b → c) of ZnS precursor with the irradiation time of electron beam.

showed discrete spots, indicating these platelets are all single nanocrystals. However, these diffraction spots were not stable under the electron beam bombardment. The initial orthodoxily arranged SAED spots slowly evolved into a hexagonal array and then finally into ploycrystalline rings. The whole process is demonstrated clearly in Figure 3. Similar phenomenon also happened for the ZnSe precursor. This phenomenon can be explained by the structures transformation of the precursors, which happened during the electron beam-induced loss of ethylenediamine molecules. The above idea was further supported by the thermogravimetric analysis. TGA results are given in Figure 4. As shown in Figure 4, the decompositions of both ZnS and ZnSe precursors begin at 230 °C and end at about 430 °C, with total weight losses of 24.3 and 18.2% for ZnS and ZnSe precursors, respectively. Assuming a chemical formula for the precursor of ZnE (E = S or Se), ZnE·*x*en (en = ethylenediamine), calculations based on the TGA results gave a value of *x* equal to about 0.5 for both of the precursors, indicating a somewhat fixed composition of the ZnE precursor. The ZnS and ZnSe precursors synthesized in procedure 2 using $ZnCl_2$ as zinc source gave almost the same TEM and TGA results as in

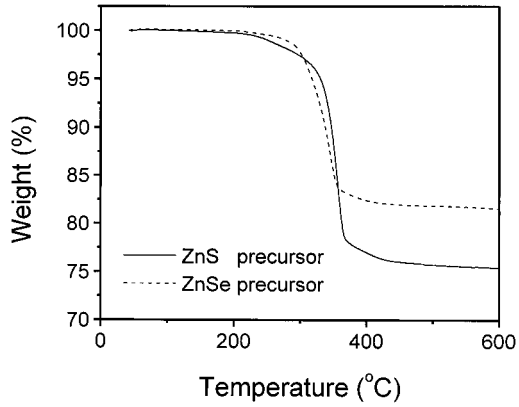

Figure 4. TGA curves of ZnS (solid line) and ZnSe (dotted line) precursors.

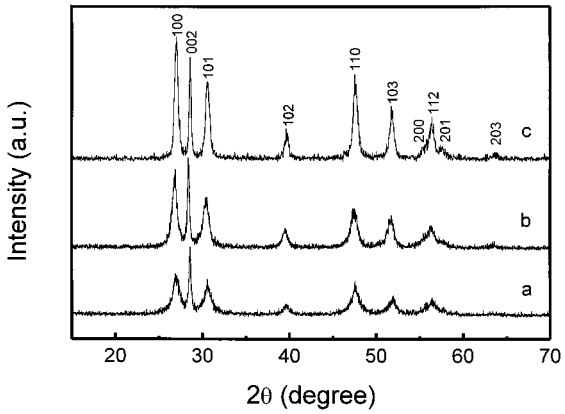

Figure 5. XRD patterns of ZnS precursor annealed in flowing argon gas at (a) 350, (b) 500, and (c) 800 °C.

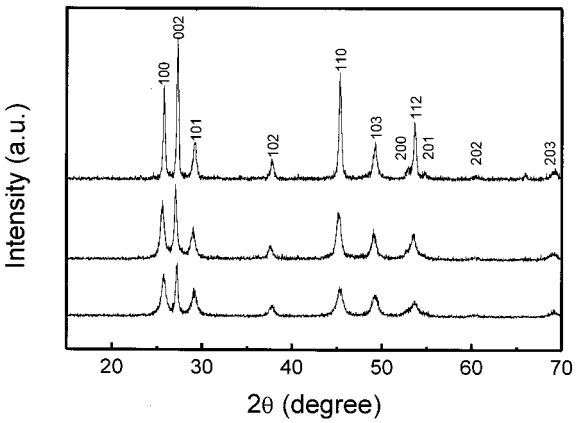

Figure 6. XRD patterns of ZnSe precursor annealed in flowing argon gas at (a) 350, (b) 500, and (c) 800 °C.

Figures 2 and 4; thus, the TEM and TGA results of these products were not given.

To determine the phase structures of the products after decomposition, these precursors were heated for 3−4 h in Ar atmosphere at different temperatures. XRD patterns of the annealed products are shown in Figures 5 and 6, which unambiguously reveal that those products are phase-pure ZnS and ZnSe with hexagonal wurtzite structures. The especially narrow and strong [002] diffraction peaks of ZnS and ZnSe products annealed at 350 or 500 °C at $2\theta = 28.5$ and 27.0°, respectively, may imply preferential growth along the 001

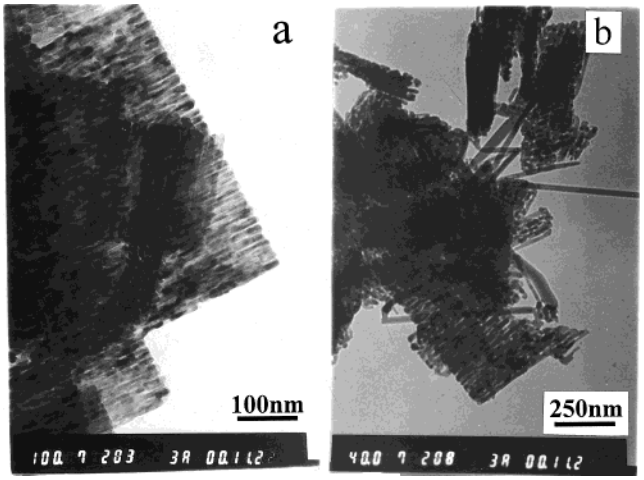

Figure 7. TEM images of (a) ZnS and (b) ZnSe products obtained by annealing the corresponding precursors at 500 °C.

direction. On the basis of the well-known Scherrer equations, the crystallite dimensions at 001 and 101 directions of the annealed products could be estimated. For ZnS, the calculated dimensions for the products annealed at 350, 500, and 800 °C are 35.3/8.8, 35.9/11.5, 36.2 nm/14.5 nm, with the numerator and denominator representing the dimensions along the 001 and 101 directions, respectively. In the case of ZnSe, these values are 29.1/13.1, 30.1/15.9, and 31.3 nm/20.3 nm correspondingly. These results are consistent with the actual TEM observations. Typical TEM images of the annealed products at 500 °C for ZnS and ZnSe precursors are shown in Figure 7, which indicate that the annealed products are predominantly small platelets with striated textures. This morphology is considered to be produced during the loss of ethylenediamine from the precursor in the annealing process. Rodlike products will be formed if these plates can further break into pieces along the textures under proper conditions. In our previous work on the preparations of CdE (E = S, Se, Te) nanoparticles, the resultant products are unexceptionally rodlike when employing ethylenediamine as a template solvent molecule. However, the loss of ethylenediamine from the platelike precursory intermediate to form individual ZnE (E = S, Se) nanorods under conventional solvothermal conditions is difficult due to the unfavorable thermodynamic and kinetic factors. As we know, the coordination ability of ethylenediamine to zinc is only slightly stronger than to cadmium (log β of $[Zn(en)_3]^{2+}$ and $[Cd(en)_3]^{2+}$ are 14.11 and 12.18, respectively). Therefore, the affinity of ethylenediamine in the inorganic framework cannot be simply analogized according to the stabilities of the corresponding metallic complex ions in aqueous solutions. In addition to the thermodynamic aspects, the kinetics of the SCMT process must be another important factor which finally caused the failure in synthesis of ZnE (E = S or Se) nanorods in ethylenediamine. Heating the precursors of ZnE under an inert atmosphere also caused the loss of ethylenediamine, but no formations of separate rodlike structures were observed. The reason can be attributed to the partial recrystallization happening during the annealing treatments, which might lead to re-interlink between the cracked parts.

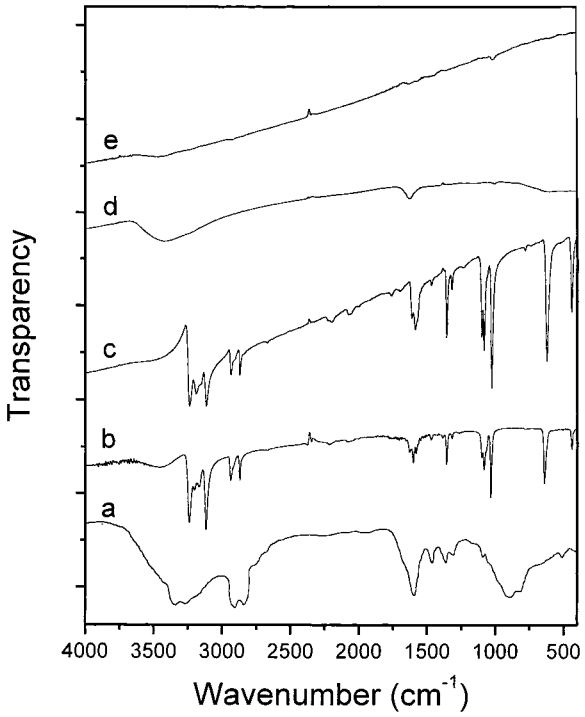

Figure 8. FTIR spectrum of ethylenediamine (a) and the as-synthesized ZnS·0.5en (b), ZnSe·0.5en (c), ZnS (d), and ZnSe (e).

Following this reason, the reduction or even disappearance of these striations should happen if higher annealing temperature or longer heating time were employed. This prediction is straightforward and was proved by TEM observations of the annealed products obtained at very high-temperature such as 800 °C, where no cracks can be observed any more. As a contrast, hydrothermal processing of elemental Zn and S or Se in an aqueous solution of NaOH only produced irregular nanoparticles with cubic zinc blende structures.

X-ray fluorescence (XRF) analysis was also utilized to determine the compositions of the precursors for ZnS and ZnSe. The XRF results indicated the ratios of Zn to S and Zn to Se in the precursors were 1.1:1 and 0.97:1, respectively, which are very close to the stoichiometric compositions of the final products, ZnS and ZnSe. The contents of C and N estimated from the XRF data are also in agreement with those calculated from the TGA results. Combustion analysis was also employed to determine the contents of C, N, and H in the ZnS and ZnSe precursors. The resulted percentages of C, H, and N are C (9.23%), H (3.24%), and N (10.7%) for ZnS precursors and C (6.97%), H (2.35%), and N (8.01%) for ZnSe precursors. These results are also consistent with the above empirical formulas: ZnS·0.5en and ZnSe·0.5en, with deviations of less than 3%. It is noteworthy that the numbers of ethylenediamine molecules in the chemical formulas of the precursors are almost the same and fixed for these two precursors synthesized using either procedure 1 or 2. These results also indicate the unsaturated coordination between Zn^{2+} and ethylenediamine in these precursors, as compared with $[Zn(en)_3]^{2+}$ in aqueous solution. However, we believe that the platelet shapes of ZnS and ZnSe precursors have inherent connections with the template effect of ethylenediamine. The platelet crystallization morphologies

of the precursors might be formed with ethylenediamine acting as connecting molecular bridges between neighboring ZnS(ZnSe) chains or layers. Direct evidence for this hypothesis must recur to structure determination based on single-crystal X-ray diffraction data, which is the target of our future research.

IR absorbance measurements (Figure 8) of the as-synthesized ZnS, ZnSe, and their precursors also provide interesting results. The IR spectra of the ZnS and ZnSe precursors in Figure 8 exhibit vibration bands corresponding to ethylenediamine molecules. Different from pure liquid-state ethylenediamine, the IR vibration peaks of ZnS and ZnSe precursors are much sharper and stronger, which signals weaker interactions and ordered arrangements of ethylenediamine molecules existing in the precursors. This phenomenon could be explained by periodic intercalations of a relatively small amount of ethylenediamine molecules into the inorganic frameworks composed of ZnS and ZnSe, which minimizes the interaction between neighboring ethylenediamine molecules and results in fixed orientations of these ethylenediamine molecules. In the IR spectra of ZnS and ZnSe precursors, the N−H stretching vibrations at frequencies above 3000 cm^{-1} all shift toward lower frequency, which might result from the chemical bonding action between Zn^{2+} and N atom. In addition, at frequencies below 1200 cm^{-1}, the IR spectra of both the precursors exhibit many differences from the pure ethylenediamine, which should be due to the ordered alignment and regular conformation of ethylenediamine molecules in the precursors, while in liquid-state ethylenediamine the orientation and conformation of the molecules are randomized due to thermal perturbation.

Conclusions

Phase-pure hexagonal wurtzite ZnS and ZnSe were prepared by annealing the corresponding precursors, which were formed by forming intercalates between ethylenediamine and ZnS(ZnSe) crystallites through a solvothermal route using ethylenediamine as solvent, in an inert atmosphere at temperatures above 350 °C. The decompositions of these precursors under the electron beam in the electron microscope were also described. Platelet morphologies of both ZnS and ZnSe precursors, which could be formularized as ZnE·0.5en with E = S or Se, were produced. Similar platelike morphologies with striated textures of the annealed products were found. The reason for the formation of striated textures in the annealed products was that ethylenediamine probably acts as connecting molecular bridges between neighboring ZnS (ZnSe) chains or layers. The role of ethylenediamine in the formations of ZnS and ZnSe precursors also provides further insights into the solvent coordination molecular template (SCMT) mechanism (*Inorg. Chem.* **1999**, *38*, 1382) advised previously in the synthesis of CdE (E = S, Se, Te) nanorods.

Acknowledgment. This work was supported by the NSFC through the national outstanding youth science fund (Grant No. 20025102) and the state key project of fundamental research in China (Grant No. G19990645-03).

IC0103502